ACS Photonics

Letter

pubs.acs.org/journal/apchd5

Nonlinear Surface Magnetoplasmonics in Kretschmann Multilayers

Ilya Razdolski,*[,†,⊥] Denys Makarov,[‡,∥] Oliver G. Schmidt,[‡] Andrei Kirilyuk,[†] Theo Rasing,[†] and Vasily V. Temnov*[,§]

[†]Institute for Molecules and Materials, Radboud University Nijmegen, 6525 AJ Nijmegen, The Netherlands

[‡]Institute for Integrative Nanosciences, IFW Dresden, 01069 Dresden, Germany

[§]Institut des Molécules et Matériaux du Mans, UMR CNRS 6283, Université du Maine, 72085 Le Mans Cedex, France

Supporting Information

ABSTRACT: Nonlinear magnetoplasmonics aims to utilize plasmonic excitations to control the mechanisms and tailor the efficiencies of nonlinear light frequency conversion at the nanoscale. We investigate the mechanisms of magnetic second-harmonic generation in hybrid gold−cobalt−silver multilayer structures, which support propagating surface plasmon polaritons at both fundamental and second-harmonic frequencies. Using magneto-optical spectroscopy in Kretschmann geometry, we show that the huge magneto-optical modulation of the second-harmonic intensity is dominated by the excitation of surface plasmon polaritons at the second-harmonic frequency, as shown by tuning the optical wavelength over the spectral region of strong plasmonic dispersion. Our proof-of-principle experiment highlights bright prospects of nonlinear magnetoplasmonics and contributes to the general understanding of the nonlinear optics of magnetic surfaces and interfaces.

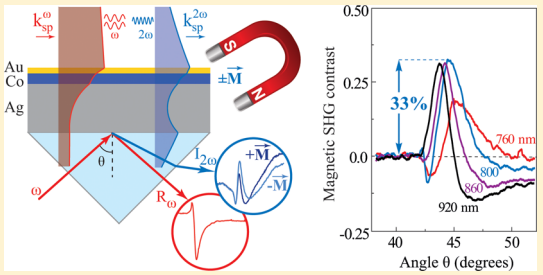

KEYWORDS: *nonlinear optics, magnetoplasmonics, surface plasmon resonance, magnetophotonics, Kretschmann geometry, nanotechnology*

Rapid development of plasmonics has facilitated an outstanding progress in understanding, designing, and controlling the optical response of metallic nanostructures, including that in the nonlinear-optical domain.[1−4] The optical second-harmonic generation (SHG) from solid interfaces represents a well-known experimental technique with numerous applications in physics, chemistry, and biology. Being a natural tool to enhance the light−matter interaction, the plasmon-assisted localization of the electric field in small volumes proved to be very effective at elevating the efficiency of nonlinear-optical processes. Beyond the physics of plasmonic nanoantennas requiring the fabrication of sophisticated metallic nanoobjects,[5,6] the Kretschmann geometry for the excitation of surface plasmon polaritons (SPPs) in a thin metallic layer on a dielectric prism plays a special role due to its robustness and simplicity.[7] A huge plasmonic enhancement of the electric field caused by the phase-matched excitation of SPPs under resonant coupling conditions has been shown to boost the SHG intensity.[8−10] The most recent experiments have evidenced that not only the SPP resonance at a fundamental frequency ω but also the excitation of a second harmonic SPP at the doubled frequency 2ω play an important role in the process of nonlinear-optical conversion.[10,11]

Here we design a nanoscale optical experiment where we could excite, detect, and manipulate the nonlinear interactions between the SPPs at the fundamental and SHG frequencies. The main idea of this study was to demonstrate the rich, yet unexplored opportunities provided by the nonlinear magnetoplasmonics. While a few works report sizable modulation of the magnetic SHG output mediated by the SPP excitation at the fundamental frequency ω only,[13−16] our experimental approach allows for the first time a direct comparison of the magnetic SHG effects driven by the SPPs excited at either ω or 2ω. We demonstrate that the SPP excitation at the SHG frequency 2ω allows enhancing the magneto-optical modulation of the SHG output significantly, thus driving the magnetic contrast up to 33%.

In this work we have adopted the concepts of linear magnetoplasmonics in hybrid metal−ferromagnet multilayer structures[3,12] together with the most recent ideas in nonlinear plasmonics.[10,11,15,17,18] Our experimental geometry is sketched in Figure 1a. A thin gold/cobalt/silver trilayer structure was grown on a glass substrate by means of the magnetron sputtering. A 5 nm thin magneto-optically active layer of ferromagnetic cobalt was protected from oxidation by a 3 nm thin layer of gold. A 25 nm thick silver layer acted as the main constituent in this hybrid plasmonic nanostructure, which was excited by collimated femtosecond laser pulses through the glass prism (Kretschmann geometry). The reflected SHG intensity, as well as the linear reflectivity signal at both fundamental ω and double frequency 2ω, was recorded as a function of the incidence angle θ for the two opposite in-plane

Received: September 8, 2015
Published: January 19, 2016

DOI: 10.1021/acsphotonics.5b00504
ACS Photonics 2016, 3, 179−183

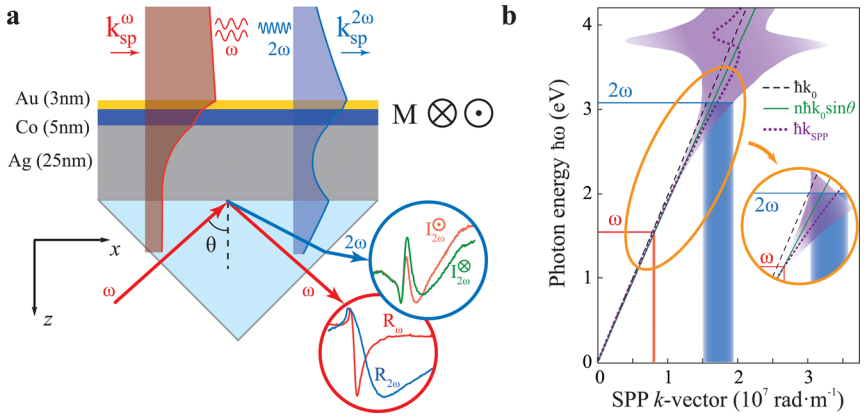

Figure 1. Surface plasmons in Au/Co/Ag multilayer structures. (a) Sketch of the experimental geometry showing the spatial distribution of the square of the normal projection of the electric field at the angles of incidence θ corresponding to the SPP excitations at the fundamental ω and double 2ω frequencies. Insets in the colored circles show the experimental angular dependencies of the linear-optical reflectivity and SHG intensities for the two opposite directions of magnetization of the cobalt layer. (b) Dispersion of the SPP in the Au/Co/Ag trilayer under study. Black dashed and green solid lines represent the photons in a vacuum and in glass, respectively. The thick dotted purple line is the calculated SPP dispersion; its line width is shown with the purple background area. The inset illustrates the possibility of a simultaneous excitation of the SPPs at both frequencies ω and 2ω. The dispersion shown here is calculated within the effective media approximation developed in ref 1. The use of this approach is justified in the Supporting Information, where these calculations are compared with the results of the finite difference time domain calculations.

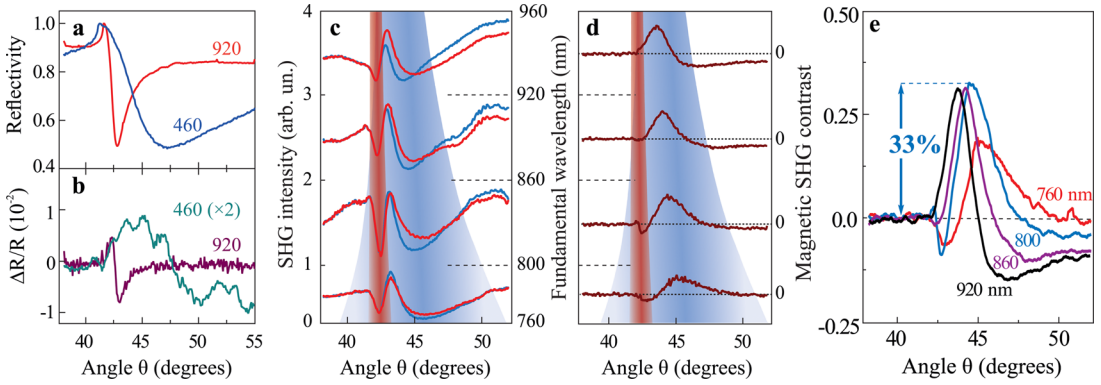

Figure 2. Angular spectra of the linear and nonlinear magneto-optical response in the presence of the SPPs. (a, b) Linear-optical reflectivity R and magnetization-induced reflectivity variations $\Delta R/R$ for the excitation with the 920 and 460 nm wavelengths. (c, d) SHG intensity and (d) mSHG contrast ρ angular spectra plotted with an offset. Red and blue background areas illustrate the SPP dispersion in the experimental spectral range (760−920 nm for the fundamental, 380−460 for the SHG, respectively.) (e) Angular spectra of the mSHG magnetic contrast ρ for the four fundamental wavelengths; no offset is introduced.

directions of magnetization (+M and − M in Figure 1a) of cobalt in the transverse Kerr geometry.

Understanding the properties of the SPP dispersion[19,20] in our structure (see Figure 1b and Supporting Information for details) is one of the key points for nonlinear magneto-plasmonics. Due to inevitable dispersion, the SPP excitations at fundamental and double frequencies in Kretschmann geometry occur at slightly different angles, suggesting that simultaneous phase-matched excitation of both SPPs is impossible. However, nonlinear-optical considerations account for the following nonlinear phase-matching condition

$$2k_0(\omega)\, n(\omega) \sin\theta_{nl} = k_{spp}(2\omega) \qquad (1)$$

between the excitation source at the silver−glass interface characterized by the in-plane component of the k-vector k_0^{ω} sin θ and the second-harmonic SPP at the gold−air interface with the k-vector $k_{spp}^{2\omega}$. Being just one of several possible SPP frequency conversion pathways,[10,21] this phase-matching condition plays a crucial role in our interpretation, as it determines the resonant SPP-induced enhancement of the nonlinear susceptibility $\chi^{(2)}$.

The experimental results are summarized in Figure 2. The linear optical reflectivities in Kretschmann configuration using the fundamental (920 nm) and second-harmonic wavelengths (460 nm, frequency doubled in a BBO crystal) are displayed in Figure 2a. A narrow plasmonic reflectivity dip at 920 nm observed at 42.5° contrasts with a much broader minimum at 460 nm at $\theta \approx 47°$, in agreement with much higher SPP losses at 2ω. In terms of linear magnetoplasmonics these two resonances behave similarly: the relative magnetization-induced variations of the reflectivity, $\Delta R/R$, neatly follow the angular differential reflectivity $dR/d\theta$, suggesting that altering the magnetization direction induces a small shift of the reflectivity spectrum due to the magnetic contribution to the SPP wavevector.[1,22]

Whereas the linear reflectivity at fundamental frequency ω shows only small modulations on the order of 1%, in line with ref 3, the SHG angular spectra at 2ω display drastic changes, as shown in Figure 2b for four different values of the fundamental wavelength 760, 800, 860, and 920 nm. Red and blue

DOI: 10.1021/acsphotonics.5b00504
ACS Photonics 2016, 3, 179−183

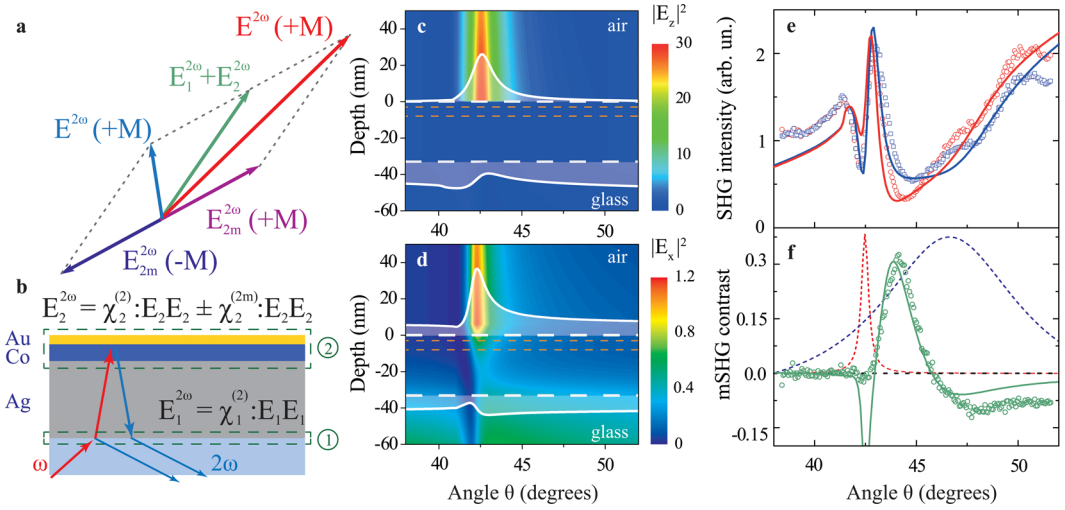

Figure 3. Schematics of the SPP-assisted mSHG generation in a multilayer structure. (a) Illustration of the origin of the inequality of the SHG intensities for the opposite direction of the external magnetic field H leading to the nonzero magnetic contrast ρ. (b) SHG sources at the two interfaces, bottom (1, glass/Ag) and top (2, air/Au/Co/Si). (c, d) False-color spatial distributions of the square of the electric field projections $|E_z|^2$ and $|E_x|^2$ at the 860 nm fundamental wavelength. Dashed white lines show the sample borders. Solid white lines represent the corresponding $|E|^2$ angular distributions at the top and bottom interfaces. (e, f) SHG intensity for the two opposite directions of the external magnetic field (red and blue symbols) and mSHG contrast angular spectra (green open circles) for the 860 nm fundamental wavelength together with the fit lines based on eq 3. Dashed lines are the angular profiles corresponding to the resonant SPP excitation at the frequency ω and nonlinear SPP excitation $\omega \rightarrow 2\omega$ (see Figure 5S in the Supporting Information).

background areas show the SPP dispersion (see Figure 1b) at the frequencies ω and 2ω, respectively, recalculated as a function of incidence angle θ. Over the SHG wavelengths range (380−460 nm) the SPP shows a strongly dispersive behavior, resulting in a shift of the resonant angle and decrease of losses (see the line width). The fundamental SPP remains nearly dispersionless and demonstrates no noticeable change of its line width. Contrary to previously reported results on a gold film,[11] the angular positions of the SPP resonances for the fundamental and SHG frequencies in our multilayer structure correspond to the pronounced minima in the SHG intensity. A strong dependence of SHG intensity on magnetization direction $I_{2\omega}(\pm M)$ is quantified by the magnetic SHG (mSHG) contrast ρ:

$$\rho = \frac{I_{2\omega}(+M) - I_{2\omega}(-M)}{I_{2\omega}(+M) + I_{2\omega}(-M)} \tag{2}$$

shown in Figure 2d. Surprisingly, the largest magnetization-induced modulation of the SHG intensity is accompanied by the SPP excitation at the SHG frequency and not the fundamental one. Angular dependence of mSHG contrast replotted in Figure 2e without an offset displays the largest reported values of modulation, reaching 33% around $\theta = 44°$. For the shortest wavelength (760 nm) the mSHG maximum is only about 20%, since in this case the SPP damping at the SHG frequency becomes so large that the system approaches the region with the nonpropagating (propagation length $\lambda^{SPP} < \lambda_{2\omega}$) SPPs. This observation links up our measurements to the most recent results by Zheng et al.,[15] who reported similar values of the mSHG contrast on a 10 nm thin iron film on glass, a structure not supporting SPPs at the SHG frequency. This fact, along with the dispersive shift of the mSHG maximum, reinforces our conclusion that the 33%, large mSHG contrast (which is equivalent to the increase of the SHG intensity by a factor of 2 upon magnetization reversal) is dominated by the SPP resonance at the SHG frequency.

In order to understand these experimental observations, we have used the approach proposed by Palomba and Novotny,[11] who explained the complex angular dependence of the SHG intensity from a thin gold film on glass by an interference of two contributions coming from the gold−air and gold−glass interfaces. In our case (Figure 3a) the silver−sapphire interface acts as a source of the nonmagnetic SHG $\vec{E}_1^{2\omega}$, and the upper part consisting of Au and Co layers is assumed to generate the electric field $\vec{E}_2^{2\omega}$ containing both magnetic $\chi^{(2m)}$ and nonmagnetic $\chi^{(2)}$ contributions. Thus, the total SHG intensity $I_{2\omega}$ is described by

$$\begin{aligned} I_{2\omega} &\propto |\vec{E}_1^{\,2\omega} + \vec{E}_2^{\,2\omega} \pm \vec{E}_{2m}^{\,2\omega}| \\ &= |\chi_1^{(2)}\vdots \vec{E}_1\vec{E}_1 + \chi_2^{(2)}\vdots \vec{E}_2\vec{E}_2 \pm \chi_2^{(2m)}\vdots \vec{E}_2\vec{E}_2|^2 \end{aligned} \tag{3}$$

where complex tensor components $\chi_1^{(2)}$ and $\chi_2^{(2)} \pm \chi_2^{(2m)}$ represent the effective optical nonlinearities at both interfaces. The angular dependences of the electric fields $\vec{E}_1$ and $\vec{E}_2$ at the fundamental frequency ω, which are driving the SHG process at both interfaces, are calculated by the finite difference time domain method for the 860 nm excitation wavelength (see Figure 3c,d).

We note that eq 3 represents an interference of the SHG electric fields from the top and the bottom interfaces, where the generation efficiency is largely determined by the angular dependence of the electric field $E(\theta)$ at the fundamental frequency. Although the excitation of SPP at the double frequency 2ω does not affect the electric fields E^{ω}, it results in a resonant contribution to the nonlinear susceptibility $\chi^{(2)}$.

Also, the magnetization reversal $M \rightarrow -M$ only slightly changes the spatial distribution of the electric field $E^{(\omega)}(z)$ and cannot induce large magnetization-induced modulation of the SHG output (see Supporting Information for details). The latter can be explained as an interference phenomenon between the magnetic contribution $\chi^{(2m)}$ from the upper (Au/Co) interface with the nonmagnetic $\chi^{(2)}$ contributions from both interfaces (Figure 3a,b).

DOI: 10.1021/acsphotonics.5b00504
ACS Photonics 2016, 3, 179−183

On the basis of these calculations, the modulation of SHG intensity in the vicinity of fundamental SPP resonance can be explained by destructive interference of two contributions, $\vec{E}_1^{2\omega}$ and $\vec{E}_2^{2\omega}$.[11] The SHG intensity minimum around the fundamental SPP resonance at $\theta = 42.5°$ can be associated with the strong increase of $\vec{E}_2$ in Figure 3c,d at the upper interface. This requires us to assume that the nonlinearity of the upper interface is smaller than the lower one. This assumption is substantiated by the independent SHG measurements without the prism coupler performed from both sides of the sample. The SHG output measured from the Ag side was several times higher than that from the Au/Co side (see Figure S4 in the Supporting Information for details). The absence of the magnetic SHG signal when probing from the Ag side proved the lack of sensitivity to the opposite interface.

The same explanation holds for the SHG minimum around $\theta = 45°$ albeit for a different reason. We note that the nonlinear susceptibility $\chi^{(2)}$ is known to acquire an SPP-induced resonant contribution, $\chi^{(2)} = \chi^{(2)}_{nr} + \chi^{(2)}_{res}$[23,24] with

$$\chi^{(2)}_{res}(\theta) \propto \frac{1}{\theta - \theta_{nl} + i\Gamma} \tag{4}$$

Owing to this resonant contribution, the SHG field enhanced at the top interface destructively interferes with the one generated at the bottom interfaces, which explains the experimentally observed SHG intensity minimum. In order to understand the angular spectrum of this resonant contribution, we approximated it with the Lorentzian resonance line. The width Γ and the angular position θ_{nl} of this resonance line was chosen according to the calculations shown in Figure 1b for the nonlinear SPP excitation at frequency 2ω, or 430 nm wavelength. This resonant shape successfully accounts for the large mSHG modulation at the angles corresponding to the nonlinear SPP excitation quantified by eq 1. On the basis of eq 3 we were able to fit the experimental angular spectra using the resonant part of the nonlinear susceptibility $\chi^{(2)}_{res}$ only.

Leaving out the details of our fitting of eq 3 for the Supporting Information, where the choice of predominant $\chi^{(2)}$ components (from the six nonzero ones, three magnetic and three nonmagnetic, at each interface) is also justified, we would like to claim to have obtained a good quantitative agreement between the theory and experiment both for angular dependence of the SHG intensity (Figure 3e) and for mSHG contrast (Figure 3f). Note that the mismatch between the experimental data and the fit curves occurs largely around the fundamental SPP resonance, where the resonant $\chi^{(2)}$ contribution used in our simulations is hardly playing any role. A more sophisticated analysis involving a large number of fit parameters[25] could potentially yield better agreement with the experimental data at the angles about 42.5°, where the SPP at ω is excited. Also, in the future it would be interesting to test the validity of our effective interface approach and thus estimate the error introduced hereby. However, such procedures are beyond the scope of this paper, which is largely focused on the large magneto-optical modulation offered by the SPP coupling at the SHG frequency.

On the basis of our numerical calculations, we can conclude that the large value (33%) of the mSHG contrast is dominated by the properties of SPP resonance at the SHG frequency. Thus, upon reversing the external magnetic field, the SHG output can be doubled, which opens up a new strategy for the design of nonlinear magnetophotonic devices operating at the nanoscale. The frequency dependence over the dispersive SPP spectral range clearly demonstrated that the maximum value of 33% mSHG contrast remains large, whereas its angular width decreases as the SHG resonance gets narrower and shifts toward the fundamental resonance.

In the given spectral range one would expect to reach further enhancement of mSHG contrast by systematically varying the individual thicknesses in this trilayer structure. The future route for investigations will imply moving toward the experiments in the telecom frequency range, which apart from the obvious technological importance would allow extending the magneto-optical investigations including the magnetization-induced third-harmonic generation. Moreover, expanding into the far-IR or THz spectral range, where the SPP dispersion is lower, would allow exploring the phase-matched magnetoplasmonic coupling between the SPPs at the fundamental and second-, third-, and higher-order harmonic frequencies. With the largest reported plasmon-assisted value of mSHG contrast of 33% we get closer to the dream of nonlinear magnetophotonic devices based on novel physical principles.

■ ASSOCIATED CONTENT

Supporting Information

The Supporting Information is available free of charge on the ACS Publications website at DOI: 10.1021/acsphotonics.5b00504.

Surface plasmon dispersion in Au/Co/Ag trilayers; linear reflectivity in the presence of SPP; nonlinear-optical SPP excitation; fitting experimental data (PDF)

■ AUTHOR INFORMATION

Corresponding Authors

*E-mail: razdolski@fhi-berlin.mpg.de.
*E-mail: vasily.temnov@univ-lemans.fr.

Present Addresses

[⊥]Phys. Chemie, Fritz-Haber-Institut der MPG, Faradayweg 4−6, 14195 Berlin, Germany.
[∥]Institute of Ion Beam Physics and Materials Research, Helmholtz-Zentrum Dresden-Rossendorf e.V., 01328 Dresden, Germany.

Notes

The authors declare no competing financial interest.

■ ACKNOWLEDGMENTS

The authors are indebted to Dr. T. V. Murzina (Moscow State University) for stimulating discussions and C. Krien (IFW Dresden) for the deposition of metal films. We thank Stratégie Internationale NNN-Telecom de la Région Pays de La Loire, Alexander von Humboldt Stiftung, the European Research Council (FP7/2007-2013)/ERC grant agreement no. 306277, and the Region Pays de La Loire for funding.

■ REFERENCES

(1) Temnov, V. V.; Armelles, G.; Woggon, U.; Guzatov, D.; Cebollada, A.; García-Martín, A.; García-Martín, J.-M.; Thomay, T.; Leitenstorfer, A.; Bratschitsch, R. Active magneto-plasmonics in hybrid metal-ferromagnet structures. *Nat. Photonics* **2010**, *4*, 107−111.

(2) Kauranen, M.; Zayats, A. V. Nonlinear plasmonics. *Nat. Photonics* **2012**, *6*, 737−748.

(3) Armelles, G.; Cebollada, A.; García-Martín, A.; González, M. U. Magnetoplasmonics: Combining magnetic and plasmonic functionalities. *Adv. Opt. Mater.* **2013**, *1*, 10−35.

DOI: 10.1021/acsphotonics.5b00504
ACS Photonics 2016, 3, 179−183

(4) Belotelov, V. I.; Kreilkamp, L. E.; Akimov, I. A.; Kalish, A. N.; Bykov, D. A.; Kasture, S.; Yallapragada, V. J.; Venu Gopal, A.; Grishin, A. M.; Khartsev, S. I.; Nur-E-Alam, M.; Vasiliev, M.; Doskolovich, L. L.; Yakovlev, D. R.; Alameh, K.; Zvezdin, A. K.; Bayer, M. Plasmon-mediated magneto-optical transparency. *Nat. Commun.* **2013**, *4*, 2128.
(5) Novotny, L.; van Hulst, N. Antennas for light. *Nat. Photonics* **2011**, *5*, 83−90.
(6) Hanke, T.; Cesar, J.; Knittel, V.; Trügler, A.; Hohenester, U.; Leitenstorfer, A.; Bratschitsch, R. Tailoring Spatiotemporal Light Confinement in Single Plasmonic Nanoantennas. *Nano Lett.* **2012**, *12* (2), 992−996.
(7) Kretschmann, E.; Raether, H. Radiative Decay of Non Radiative Surface Plasmons Excited by Light. *Z. Naturforsch., A: Phys. Sci.* **1968**, *23*, 2135−2136.
(8) Simon, H. J.; Mitchell, D. E.; Watson, J. G. Optical second-harmonic generation with surface plasmons in silver films. *Phys. Rev. Lett.* **1974**, *33*, 1531−1534.
(9) Naraoka, R.; Okawa, H.; Hashimoto, K.; Kajikawa, K. Surface plasmon resonance enhanced second-harmonic generation in Kretschmann configuration. *Opt. Commun.* **2005**, *248*, 249−256.
(10) Grosse, N. B.; Heckmann, J.; Woggon, U. Nonlinear plasmon-photon interaction resolved by k-space spectroscopy. *Phys. Rev. Lett.* **2012**, *108*, 136802.
(11) Palomba, S.; Novotny, L. Nonlinear excitation of surface plasmon polaritons by four-wave mixing. *Phys. Rev. Lett.* **2008**, *101*, 056802.
(12) Temnov, V. V. Ultrafast acousto-magneto-plasmonics. *Nat. Photonics* **2012**, *6*, 728−736.
(13) Razdolski, I.; Gheorghe, D. G.; Melander, E.; Hjörvarsson, B.; Patoka, P.; Kimel, A. V.; Kirilyuk, A.; Papaioannou, E. Th.; Rasing, Th. Nonlocal nonlinear magneto-optical response of a magnetoplasmonic crystal. *Phys. Rev. B: Condens. Matter Mater. Phys.* **2013**, *88*, 075436.
(14) Chekhov, A. L.; Krutyanskiy, V. L.; Shaimanov, A. N.; Stognij, A. I.; Murzina, T. V. Wide tunability of magnetoplasmonic crystals due to excitation of multiple waveguide and plasmon modes. *Opt. Express* **2014**, *22*, 17762−17768.
(15) Zheng, W.; Hanbicki, A.; Jonker, B. T.; Lüpke, G. Control of magnetic contrast with nonlinear magneto-plasmonics. *Sci. Rep.* **2014**, *4*, 1−5.
(16) Krutyanskiy, V. L.; Chekhov, A. L.; Ketsko, V. A.; Stognij, A. I.; Murzina, T. V. Giant nonlinear magneto-optical response of magnetoplasmonic crystals. *Phys. Rev. B: Condens. Matter Mater. Phys.* **2015**, *91*, 121411(R).
(17) Krutyanskiy, V. L.; Kolmychek, I. A.; Gan'shina, E. A.; Murzina, T. V.; Evans, P.; Pollard, R.; Stashkevich, A. A.; Wurtz, G. A.; Zayats, A. V. Plasmonic enhancement of nonlinear magneto-optical response in nickel nanorod metamaterials. *Phys. Rev. B: Condens. Matter Mater. Phys.* **2013**, *87*, 035116.
(18) Razdolski, I.; Parchenko, S.; Stupakiewicz, A.; Semin, S.; Stognij, A. I.; Maziewski, A.; Kirilyuk, A.; Rasing, Th. Second-Harmonic Generation from a Magnetic Buried Interface Enhanced by an Interplay of Surface Plasma Resonances. *ACS Photonics* **2015**, *2*, 20−26.
(19) Dionne, J. A.; Sweatlock, L. A.; Atwater, H. A.; Polman, A. Planar metal plasmon waveguides: frequency-dependent dispersion, propagation, localization, and loss beyond the free electron model. *Phys. Rev. B: Condens. Matter Mater. Phys.* **2005**, *72*, 075405.
(20) Foley, J. J., IV; Harutyunyan, H.; Rosenmann, D.; Divan, R.; Wiederrecht, G. P.; Gray, S. K. When are Surface Plasmon Polaritons Excited in the Kretschmann-Raether Configuration? *Sci. Rep.* **2015**, *5*, 9929.
(21) Heckmann, J.; Kleemann, M.-E.; Grosse, N. B.; Woggon, U. The dual annihilation of a surface plasmon and a photon by virtue of a three-wave mixing interaction. *Opt. Express* **2013**, *21*, 28856−28861.
(22) González-Díaz, J. B.; García-Martín, A.; Armelles, G.; García-Martín, J.-M.; Clavero, C.; Cebollada, A.; Lukaszew, R. A.; Skuza, J. R.; Kumah, D. P.; Clarke, R. Surface-magnetoplasmon nonreciprocity effects in noble-metal/ferromagnetic heterostructures. *Phys. Rev. B: Condens. Matter Mater. Phys.* **2007**, *76*, 153402.
(23) Raschke, M.; Hayashi, M.; Lin, S.; Shen, Y. Doubly-resonant sum-frequency generation spectroscopy for surface studies. *Chem. Phys. Lett.* **2002**, *359*, 367−372.
(24) Heinz, T. F. Second-order nonlinear optical effects at surfaces and interfaces. In *Nonlinear Surface Electromagnetic Phenomena*; Ponath, H.-E., Stegeman, G. I., Eds.; Elsevier: Amsterdam, 1991.
(25) Pavlov, V. V.; Tessier, G.; Malouin, C.; Georges, P.; Brun, A.; Renard, D.; Meyer, P.; Ferre, J.; Beauvillain, P. Observation of magneto-optical second-harmonic generation with surface plasmon excitation in ultrathin Au/Co/Au films. *Appl. Phys. Lett.* **1999**, *75*, 190−192.

DOI: 10.1021/acsphotonics.5b00504
ACS Photonics 2016, 3, 179−183